

Model-based real-time control of a magnetic manipulator system

Damsteeg, Jan Willem; Nagesh Rao, Subramanya P.; Babuška, Robert

DOI

[10.1109/CDC.2017.8264140](https://doi.org/10.1109/CDC.2017.8264140)

Publication date

2017

Document Version

Final published version

Published in

Proceedings 2017 IEEE 56th Annual Conference on Decision and Control (CDC 2017)

Citation (APA)

Damsteeg, J. W., Nagesh Rao, S. P., & Babuška, R. (2017). Model-based real-time control of a magnetic manipulator system. In *Proceedings 2017 IEEE 56th Annual Conference on Decision and Control (CDC 2017)* (pp. 3277-3282). IEEE. <https://doi.org/10.1109/CDC.2017.8264140>

Important note

To cite this publication, please use the final published version (if applicable). Please check the document version above.

Copyright

Other than for strictly personal use, it is not permitted to download, forward or distribute the text or part of it, without the consent of the author(s) and/or copyright holder(s), unless the work is under an open content license such as Creative Commons.

Takedown policy

Please contact us and provide details if you believe this document breaches copyrights. We will remove access to the work immediately and investigate your claim.

Model-based real-time control of a magnetic manipulator system

Jan-Willem Damsteeg¹, Subramanya P. Nageshroo², and Robert Babuška¹

Abstract—Precise magnetic manipulation has numerous applications, ranging from manufacturing to the medical field. Owing to the nonlinear nature of the electromagnetic force, magnetic manipulation requires advanced nonlinear control. In this paper, we design and experimentally evaluate two nonlinear controllers for a magnetic manipulation (Magman) system, which consists of four electromagnetic coils arranged linearly. The current through the coils is controlled in order to accurately position a steel ball, rolling freely in a track above the coils. We benchmark two nonlinear control methods, namely feedback linearization and a constrained state-dependent Riccati equation (SDRE) control. These methods are chosen due to their widespread use in academia as well as industrial applications. On the actual setup, constrained SDRE has performed considerably better in terms of the settling time, overshoot, and the amount of control effort when compared to feedback linearization.

I. INTRODUCTION

Magnetic manipulation is a concept where feedback-controlled electromagnets dynamically shape a magnetic field in order to place a magnetic object at a desired position or move it along a desired trajectory. The use of electromagnetic force allows for contact-less manipulation, micro-object handling and precise positioning of objects. This approach has diverse applications primarily in difficult to access or dangerous environments, in situations where a mechanical gripper cannot be used [1], [2], [3], or in applications which require contactless, high precision positioning [4]. Another active research field are medical procedures that involve untethered navigation and manipulation of objects inside human or animal body, such as non-invasive surgery, remote delivery of drugs, etc. For a brief overview of existing methods see [5], [6], [7] and the references therein. Recently in [8], [9], the authors have introduced a novel methodology that can selectively actuate either an individual object or a collection of objects.

In this paper, we benchmark two model-based nonlinear control methods on a magnetic manipulator setup called Magman, see Fig. 1. The Magman system has four electromagnetic coils arranged linearly. By actively controlling the current through the coils, the magnetic field above them can be shaped to manipulate a magnetic object – a steel ball in our case ($m = 0.032$ kg). The control objective is to position/regulate the ball quickly, accurately, and without overshoot. As the magnetic force exerted on the ball is a highly nonlinear and uncertain function of the electric

current and the ball position, advanced control methods are required (for details see [10], [11]). In addition, owing to the construction of the track on which the ball rolls, the frictional forces are negligible and so is the internal damping in the system.



Fig. 1. The Magman setup consists of four electromagnetic coils. By individually controlling the current through each coil, a steel ball can be positioned along a track above the coils. The position of the ball is measured by a laser sensor that is placed at the left side of the setup.

A schematic of the setup is given in Fig. 2.

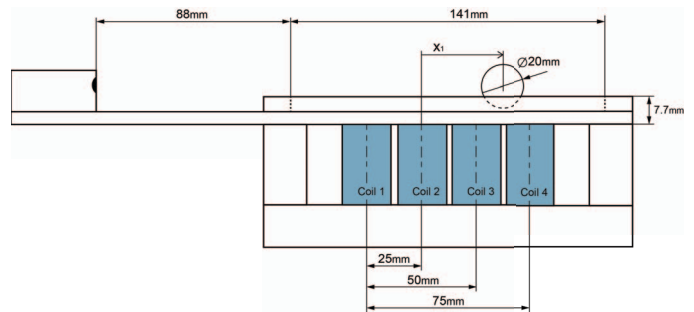


Fig. 2. A schematic of the Magman setup with the dimensions.

The current through each coil is controlled by PWM (pulse-width modulated) signal using custom made control boards, communicating with the PC through a serial connection, using the RS232 protocol. The position of the ball is measured by using a laser scanner (Micro-Epsilon, Opto 1301) [12]. The scanner has a range of 200 mm at a maximum sampling frequency of 1000 Hz. The position data are acquired by using a data acquisition board (Humusoft MF624).

This paper is organized as follows; in Section 2, a mathematical model of the magman (see Fig. 1) is given, also parameters of the system are identified. In Section 3 two well known nonlinear control methods namely, feedback linearization and constrained SDRE are evaluated. Here the objective is to demonstrate the application of advanced control methods for realtime control of a complex nonlinear system. First the controllers are tuned in simulation and

¹ Cognitive Robotics department, Delft University of Technology, Mekelweg 2, 2628 CD Delft, The Netherlands. j-w@online.nl, r.babuska@tudelft.nl

² Research & Advanced Engineering, Ford Motor Company, 2101 Village Rd, Dearborn, MI 48124, USA. snageshr@ford.com

then later re-tuned on the setup. Conclusions are given in Section 4 with a note on planned future work.

II. MODELING AND SYSTEM IDENTIFICATION

The force profile of a magnetic coil similar to the one used in Fig. 1 was obtained in [10]. The force on the ball was measured using a force gauge and its position can be measured either using laser scanner, resistive foil or overhead camera. From the measured data a functional relation between the force, current through the coil, and the distance between the ball to the center of the coil can be found. An analytical expression of electromagnetic force on the steel ball due to a single coil is (for details see [13])

$$F(x, I) = g(x) I = \frac{-\alpha x}{(x^2 + \beta)^3} I \quad (1)$$

where $x \in \mathbb{R}$ is the distance between the ball to the center of the coil, α and β are the dimensionless coil parameters, and $I \in \mathbb{R}$ is the current through the coil. A 3-d surface plot of (1) is given in Fig. 3.

The translational force in (1) is obtained by simplifying the classical force equation which is a function of I^2 , see [14]. Our approximation in (1) can be attributed to the small region of operation of the used coils (Fig. 1), and is also verified by the experimental validation.

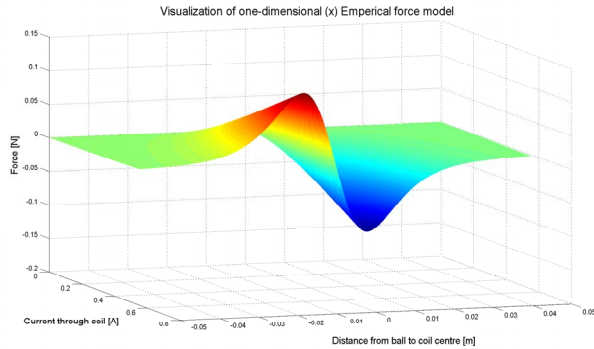


Fig. 3. Magnetic force exerted on the ball as a function of its distance to the coil, see equation (1).

A. Continuous-time state space model

Using (1), the equations of motion for the steel ball on an one dimensional array of magnetic coils (see Fig. 1) is

$$\dot{X} = \begin{bmatrix} \dot{x} \\ \ddot{x} \end{bmatrix} = \begin{bmatrix} \dot{x} \\ -\frac{b}{m} \dot{x} + \frac{1}{m} \sum_{j=1}^4 g(x, j) I_j \end{bmatrix} \quad (2)$$

where $X = (x, \dot{x})^T$ is the continuous time state vector consisting of position x and velocity \dot{x} of a steel ball of mass m . In (2), $g(x, j)I_j$ is the magnetic force exerted by coil j which is dependent on the position x of the ball and is given by,

$$g(x, j) = \frac{-\alpha (x - 0.025 \times j)}{(x - 0.025 \times j)^2 + \beta)^3} \quad (3)$$

where control input I_j is the current through the coil j , for $j \in \{1, 2, 3, 4\}$. The nonlinear magnetic force function in (3) is a modification of (1) for an array of coils.

The nonlinear dynamics of the steel ball (2) can be written in state dependent coefficient (SDC) form as

$$\dot{X} = \underbrace{\begin{bmatrix} 0 & 1 \\ 0 & -\frac{b}{m} \end{bmatrix}}_A X + \underbrace{\begin{bmatrix} 0 & 0 & 0 & 0 \\ \frac{g(x,1)}{m} & \frac{g(x,2)}{m} & \frac{g(x,3)}{m} & \frac{g(x,4)}{m} \end{bmatrix}}_{B(X)} u \quad (4)$$

where $u = (I_1, I_2, I_3, I_4)^T$ is the current through the four coils, respectively. The position of the ball x is measured using μE -optoNCDT laser sensor, the resulting output equation is

$$y = \begin{bmatrix} 1 & 0 \end{bmatrix} X. \quad (5)$$

For real-time control the continuous time model (4) needs to be discretized and is detailed in Section 3.

B. System identification of magnetic manipulator

The coil parameters α , β , and the friction coefficient b of (4) are obtained by using system identification [15]. In this paper we assume the parameters α and β to be uniform for all the four coils. This would simplify the identification process as only three parameters have to be identified, which can be estimated using nonlinear optimization algorithm `lsqnonlin` in Matlab. The optimization objective is to find numerical values for α , β and b such that the least-square error between the response on the experimental setup and the model (4) is minimized.

It must be noted that the coil cannot exert a repelling force on the ball. Also due to lack of friction the ball would roll from one end of track to the other, thus open-loop identification is not feasible. Hence closed-loop identification is done using a PD controller. For the closed loop identification a step signal with varying step size is used as a reference. For the experimental data, position was measured using the laser sensor and backward difference is used to estimate the velocity. The performance of the resulting (closed-loop) identified model was evaluated using Variance-Accounted-For (VAF) [16], and is given in Fig.4. A higher VAF value indicates the better prediction of the model parameters.

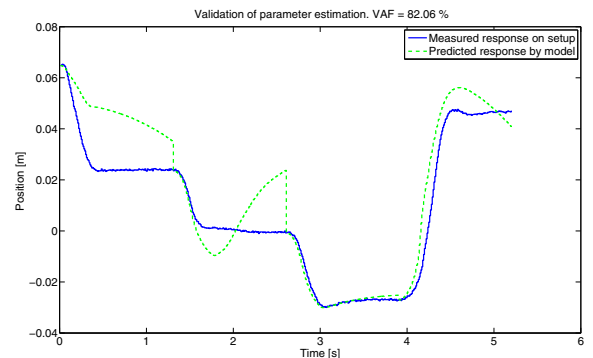


Fig. 4. Validation result, obtained VAF value for closed-loop identification is 82.06%.

The identified magman model parameters are, $\alpha = 5.52$, $\beta = 1.75$ and $b = 0.0161$. The large fluctuations around the second coil and the resulting high prediction error can be attributed to the simplified magman model in (4) and to the closed-loop identification where same control parameters are used for all the coils. Additionally, as discussed in section II, the chosen magnetic force model (4) is linear in the current, however as per standard approaches the force is a function of I^2 , this may have influenced the response in Fig.4.

A complex and an accurate model of the magman system (Fig.1) can be obtained either analytically by using first principles or numerically by using finite element methods. In many scenarios these approaches can be time consuming and expensive. In this paper, the inaccuracy due to simplified model and parameter identification is addressed by using two well known nonlinear control methods. This is further detailed in the following sections.

III. MODEL BASED CONTROL OF MAGNETIC MANIPULATOR

A. Discretization of continuous time model

For real-time computer control (4) must be discretized

$$\begin{aligned} X(k+1) &= A_d X(k) + B_d(X) u(k) \\ y(k) &= C_d X(k) + D_d u(k) \end{aligned} \quad (6)$$

where A_d , B_d , the discrete-time version of the continuous-time matrices A and B are obtained using

$$A_d = e^{AT}, \quad B_d(X) = \int_0^T e^{A^t} dt B(X) \quad (7)$$

where T is the sampling time. The system matrix A_d can be determined offline, as it is independent of X . Whereas, the input matrix $B_d(X)$ must be computed at each time step based on the current system state X . We use the Taylor series approximation for the fast and real-time computation of $B_d(X)$ ¹

$$B_d(X) = (T + AT + \frac{1}{2!}A^2T^2 + \frac{1}{3!}A^3T^3 + \frac{1}{4!}A^4T^4)B(X) \quad (8)$$

In order to reduce cluttering of symbols we have used the same notation X to represent both the continuous and discrete time state vector (see (4) and (6)).

B. Feedback Linearization

In Feedback Linearization (FL) a nonlinear system is transformed into a linear form. By using a combination of state transformations and inverse model the system nonlinearities are cancelled by the inner feedback signal. This results in linearization of the original nonlinear system. Once linearized, any suitable linear control method can be used to achieve the desired control objective. Thanks to its plainness FL is used in large number of applications. In this work we

¹If system matrix A is full rank then $B_d(X)$ can be obtained by using $B_d(X) = A^{-1}(A_d - I)B(X)$.

use *input-state* linearization approach, for other methods and examples see [17], [18], [19].

For the magnetic manipulator system (4) the feedback linearization input is

$$u_j = \frac{m}{4g(x, j)} \left(\frac{b}{m} \dot{x} + v \right), \quad (9)$$

where v is the new control input that needs to be designed by the engineer.

From (3), the magnetic force on the steel ball exerted by coil j when it is at the center of the coil is zero (see Fig. 3). Hence the singularity in (9) can be avoided by using the pseudo inverse of $g(x, j)$.

Using (9) in (4)

$$\begin{aligned} \ddot{x} &= -\frac{b}{m} \dot{x} + \frac{1}{m} \sum_{j=1}^4 g(x, j) u_j \\ &= -\frac{b}{m} \dot{x} + \frac{1}{m} \sum_{j=1}^4 g(x, j) \frac{m}{4g(x, j)} \left(\frac{b}{m} \dot{x} + v \right) \\ &= -\frac{b}{m} \dot{x} + \left(\frac{b}{m} \dot{x} + v \right) = v. \end{aligned} \quad (10)$$

An optimal state feedback controller $v = -KX$, with $K = [k_1, k_2]^T$ can be used to stabilize the system. The resulting closed-loop is

$$\dot{X} = \begin{bmatrix} 0 & 1 \\ -k_1 & -k_2 \end{bmatrix} X. \quad (11)$$

The closed loop poles of (11), also (4), are determined by the choice of k_1 and k_2 . In (11), instead of LQR any alternative linear controller such as PD can be used, however, in this work, LQR is chosen as we can constrain the control effort.

Feedback linearization can be an efficient method only if the system model is sufficiently accurate and invertible. If these conditions are not satisfied or partially satisfied then it would be difficult to achieve the desired control objective [20].

1) *FL simulation results:* The feedback control law (9) with $v = -KX$ is used to stabilize the system (4) at a desired state of $[x, \dot{x}]^T = [0, 0]^T$. The feedback gain K is obtained by solving an LQR problem (see [21]) with weight matrices chosen as $Q = \text{diag}(90, 1)$ and $R = 1e - 4$.

The resulting simulated response is given in Fig. 5. In this paper we chose, rise time, settling time and overshoot² as the performance measure criteria to evaluate different feedback controllers. The performance criteria for the simulated response of feedback linearization is given in Table. I.

TABLE I
PERFORMANCE CRITERIA OF FL CONTROLLER (9) IN SIMULATION

FL performance	
Rise time [s]	0.24
Settling time [s]	0.43
Overshoot [%]	$\simeq 0$

²for definitions see [22]

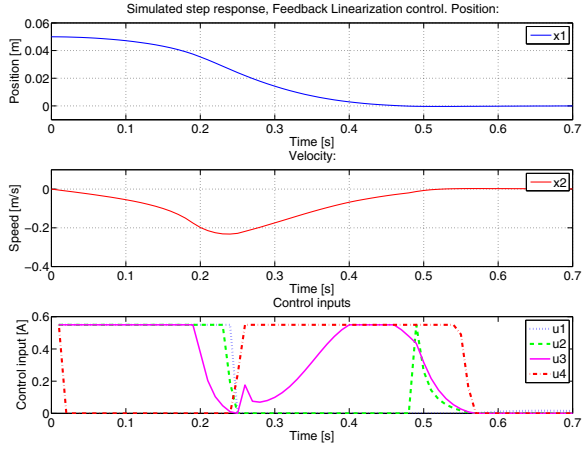


Fig. 5. Simulated response for FL controller (9) from an initial state of $[x, \dot{x}]^T = [0.05, 0]^T$ to a desired state of $[x, \dot{x}]^T = [0, 0]^T$.

From Table I it is evident that in simulation, the response of magnetic manipulator system is considerably fast with negligible overshoot. However, a major drawback of FL for magman system is that the controller (9) equalizes the effort across all the actuators irrespective of the position of the ball. This may result in large control effort and inefficient use of the magnetic field.

2) *FL on the experimental setup*: For the experimental evaluation of the magnetic manipulator (Fig. 2), the feedback controller used in simulation is chosen as initial controller.

The realtime control of the magnetic manipulator Fig. 2 is done at a sampling frequency of 100 Hz. The feedback controller (9) with $v = -KX$ is used for experimental evaluation. The LQR tuning parameters $Q = \text{diag}(33, 1)$ and $R = 1e - 4$ are used to obtain the optimal state feedback gain K . The resulting response and the corresponding control input are given in Fig.6, and the controller performance is given in Table II.

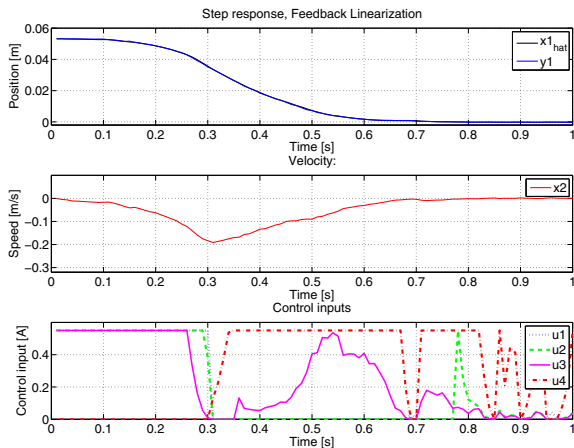


Fig. 6. Response of FL on experimental setup.

TABLE II

PERFORMANCE OF FL CONTROLLER (9) ON THE EXPERIMENTAL SETUP

Controller:	FL
Rise time [s]	0.31
Settling time [s]	0.64
Overshoot [%]	≤ 1
Control Effort [J]	21.4

From Table II, the realtime control of magman using feedback linearization has a desirable performance. When compared to the simulation results in Table I, experimental evaluation has longer settling time and almost negligible overshoot. This can be attributed to the choice of tuning parameters.

C. Constrained State Dependent Riccati Equation control - MPC approach

In state dependent riccati equation (SDRE) method the algebraic-riccati-equation (ARE) is solved online for a state-dependent-coefficient (SDC) system (2). For an introduction to SDRE see [23], [24], [25] and the reference therein. A major drawback in using SDRE is, when the control inputs are bounded due to saturation, classical solutions may result in suboptimal control. This issue can be addressed by augmenting model predictive control (MPC) with the principles of SDRE. This is known as constrained-SDRE for details see [26]. In this section we perform real-time evaluation of magman using constrained SDRE controller.

In model predictive control, the objective is to find an optimal input $u^*(0), u^*(1), \dots, u^*(N_p)$ so as to minimize a cost function [27]

$$J(X(0), \bar{U}) = \sum_{j=0}^{N_p} \left(X(j)^T Q X(j) + u(j)^T R u(j) \right), \quad (12)$$

where $\bar{U} = [u(0) \ u(1) \ \dots \ u(N_p - 1)]$ is the control input and N_p is the prediction horizon. Cost function (12) can be reformulated as (see [26])

$$J(X(0), \bar{U}) = X^T(0) Q X(0) + \bar{X}^T \bar{Q} \bar{X} + \bar{U}^T \bar{R} \bar{U} \quad (13)$$

where $\bar{X} = [X(1) \ X(2) \ \dots \ X(N_p)]$, $\bar{Q} = \text{diag}[Q \ Q \ \dots \ Q]$, and $\bar{R} = \text{diag}[R \ R \ \dots \ R]$. Using (2) the state evolution is

$$\begin{bmatrix} X(1) \\ X(2) \\ \vdots \\ X(N_p) \end{bmatrix} = \underbrace{\begin{bmatrix} B & 0 & \dots & 0 \\ AB & B & \dots & 0 \\ \vdots & \vdots & \ddots & \vdots \\ A^{N_p-1}B & A^{N_p-2}B & \dots & B \end{bmatrix}}_{\bar{S}} \begin{bmatrix} u(0) \\ u(1) \\ \vdots \\ u(N_p - 1) \end{bmatrix} + \underbrace{\begin{bmatrix} A \\ A^2 \\ \vdots \\ A^{N_p} \end{bmatrix}}_{\bar{T}} X(0) \quad (14)$$

By using (14) in (13) the cost function can be reformulated as

$$\begin{aligned}
 J(X(0), \bar{U}) &= \left(\bar{S}\bar{U} + \bar{T}X(0) \right)^T \bar{Q} \left(\bar{S}\bar{U} + \bar{T}X(0) \right) \\
 &+ X^T(0)QX(0) + \bar{U}^T \bar{R}\bar{U} \\
 &= \frac{1}{2} \bar{U}^T \underbrace{2 \left(\bar{R} + \bar{S}^T \bar{Q} \bar{S} \right)}_H \bar{U} + \underbrace{X(0)^T 2 \bar{T}^T \bar{Q} \bar{S}}_{c^T} \bar{U} + \\
 &\frac{1}{2} X(0)^T \underbrace{2 \left(Q + \bar{T}^T \bar{Q} \bar{T} \right)}_Y X(0)
 \end{aligned} \tag{15}$$

the last term $\frac{1}{2}X(0)YX(0)$ in (15) is independent of the optimization variable $u(k)$. For the remaining components the optimization problem can be formulated as a quadratic programming problem

$$\min_{\bar{U}} \frac{1}{2} \bar{U}^T H \bar{U} + c^T \bar{U} \quad \text{subject to } \bar{A}\bar{U} \leq \bar{b} \tag{16}$$

where H and c are defined in (15), \bar{U} the optimization variable, \bar{A} and \bar{b} are the inequality constraints dictated by the physical system. This QP problem can be solved in Matlab using `quadprog`, with the trust-region-reflective algorithm. However, owing to the high nonlinearity of the magnetic manipulator system (Fig.1), solving the constrained optimization problem (16) in real-time can be difficult. In this work we address this issue by combining the concepts of SDRE with the QP problem (16). By using (4) we get state dependent matrices H and c . Computing these matrices at real-time can be computationally expensive. Hence we first calculate H and c off-line, and then use the resulting look-up table to obtain appropriate parameters depending on the measured state X .

1) *C-SDRE simulation results:* The system is initialized at $x(0) = 0.05$ m, the desired set point is the origin. The control parameters are tuned for satisfactory closed-loop performance in terms of rise time, overshoot, and settling time. By using the following MPC parameters

$$Q = \begin{bmatrix} 45 & 0 \\ 0 & 0.24 \end{bmatrix} \quad R = \begin{bmatrix} 0.002 & 0 & 0 & 0 \\ 0 & 0.002 & 0 & 0 \\ 0 & 0 & 0.002 & 0 \\ 0 & 0 & 0 & 0.002 \end{bmatrix}$$

for a prediction horizon $N_p = 15$, the obtained system response and the measured performance are in Fig. 7 and Table III, respectively.

TABLE III
SIMULATION PERFORMANCE OF C-SDRE (MPC) CONTROLLER

C-SDRE performance	
Rise time [s]	0.23
Settling time [s]	0.41
Overshoot [%]	≤ 2
Control Effort [J]	8.0

As the control constraints are embedded in C-SDRE formulation (16), it gives better performance than feedback-linearization. From Table I and Table III, it is evident that the

C-SDRE controller outperforms the FL controller in terms of rise time and settling time. Furthermore, the required control effort in C-SDRE is lesser than FL controller.

2) *C-SDRE on the experimental setup:* In this section the C-SDRE method is implemented on the experimental setup. Calculating H and c at each time step and then solving the QP problem (16) can be computationally expensive. We address this issue by computing H and c matrices offline and using it as a look-up table. Only the QP problem (16), is solved online as it depends on both system states. For the experimental evaluation the penalties on both the velocity and the control inputs are increased to achieve lower overshoot and a smooth behaviour. Using the following control parameters

$$Q = \begin{bmatrix} 45 & 0 \\ 0 & 0.4 \end{bmatrix} \quad R = \begin{bmatrix} 0.006 & 0 & 0 & 0 \\ 0 & 0.006 & 0 & 0 \\ 0 & 0 & 0.006 & 0 \\ 0 & 0 & 0 & 0.006 \end{bmatrix}$$

for a prediction horizon $N_p = 15$, the obtained step response and the measured performance are in Fig. 8 and Table IV, respectively.

TABLE IV
CONTROL PERFORMANCE OF C-SDRE ON EXPERIMENTAL SETUP

Controller:	C-SDRE
Rise time [s]	0.30
Settling time [s]	0.57
Overshoot [%]	≈ 0
Control Effort [J]	6.9

From Table IV, C-SDRE controller performs relative better than FL controller. For this setup, C-SDRE is the fast, accurate, and efficient controller.

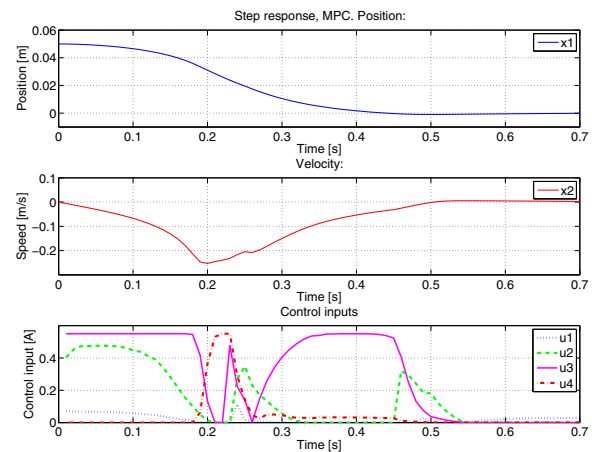


Fig. 7. Simulated step response of the Constrained-SDRE control [26] which applies the MPC concept to take the lower and upper bound constraints into account. During each time step the model is linearized, based on which the optimal control sequence is determined for the next N_p time steps, the control horizon.

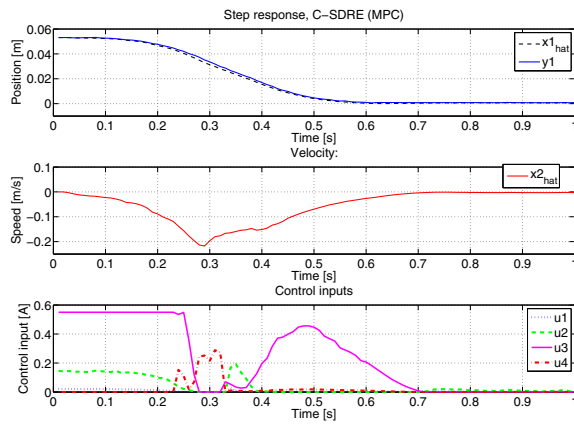


Fig. 8. Response of C-SDRE on experimental setup.

IV. CONCLUSIONS

In this paper we have performed experimental evaluation and comparison of two nonlinear controllers, namely feedback linearization and a C-SDRE controller on a magnetic manipulation (magman) system. The obtained controller performances are given in Table V.

TABLE V
PERFORMANCE OF THE TWO MODEL-BASED CONTROLLERS ON THE
EXPERIMENTAL SETUP

Controller:	FL	C-SDRE
Rise time [s]	0.31	0.30
Settling time [s]	0.64	0.57
Overshoot [%]	≤ 1	0
Control Effort [J]	21.4	6.9

Compared to the simulation results both controllers are relatively slower on the setup. The FL controller on setup requires an additional settling time of nearly 0.2 seconds compared to the simulation. Although the C-SDRE is also significantly slower than in simulation, it outperforms the FL controller on other criteria such as overshoot which is nearly zero.

A major drawback of the model-based methods evaluated in this work is their dependency on the system model. Any change in the mass of the object, a different coil, or a inclined placement of the setup may require retuning of the controller. This can be addressed by using advanced approaches namely: robust control [28], adaptive control [29], and learning control [30]. These and other relevant methods will be explored in our future work.

REFERENCES

[1] A. A. Solovev, S. Sanchez, M. Pumera, Y. F. Mei, and O. G. Schmidt, "Magnetic control of tubular catalytic microbots for the transport, assembly, and delivery of micro-objects," *Advanced Functional Materials*, vol. 20, no. 15, pp. 2430–2435, 2010.

[2] R. Pieters, S. Lombriser, A. Alvarez-Aguirre, and B. J. Nelson, "Model predictive control of a magnetically guided rolling microrobot," *IEEE Robotics and Automation Letters*, vol. 1, no. 1, pp. 455–460, 2016.

[3] A. G. Alleyne, S. Schurle, A. Meo, and B. J. Nelson, "Motion control for magnetic micro-scale manipulation," in *Control Conference (ECC), 2013 European*. IEEE, 2013, pp. 784–790.

[4] M. Khamesee and E. Shameli, "Regulation technique for a large gap magnetic field for 3d non-contact manipulation," *Mechatronics*, vol. 15, no. 9, pp. 1073–1087, 2005.

[5] B. J. Nelson, H. Marino, and C. Bergeles, "Robust h-infinity control for electromagnetic steering of microrobots," ETH, Zurich, Tech. Rep., 2012.

[6] B. Veron, A. Hubert, J. Abadie, N. Andreff, and P. Renaud, "Advocacy for multi mobile coil magnetic manipulation in active digestive endoscopy," in *IEEE/RSJ International Conference on Intelligent Robots and Systems, IROS'12.*, 2012, pp. 2–pages.

[7] S. Martel, J.-B. Mathieu, O. Felfoul, A. Chanu, E. Aboussouan, S. Tamaz, P. Pouponneau, L. Yahia, G. Beaudoin, G. Soulez, *et al.*, "Automatic navigation of an untethered device in the artery of a living animal using a conventional clinical magnetic resonance imaging system," *Applied physics letters*, vol. 90, no. 11, p. 114105, 2007.

[8] J. Rahmer, C. Stehning, and B. Gleich, "Spatially selective remote magnetic actuation of identical helical micromachines," *Science Robotics*, vol. 2, no. 3, p. eaal2845, 2017.

[9] S. Martel, "Beyond imaging: Macro- and microscale medical robots actuated by clinical mri scanners," *Science Robotics*, vol. 2, no. 3, p. eaam8119, 2017.

[10] Z. Hurak and J. Zemanek, "Feedback linearization approach to distributed feedback manipulation," in *American control conference*, Montreal, Canada, 2012.

[11] J. Zemanek, S. Celikovskiy, and Z. Hurak, "Time-optimal control for bilinear nonnegative-in-control systems: Application to magnetic manipulation," in *20th world congress, IFAC*, Toulouse, 2017, pp. 16 602–16 609.

[12] Micro-Epsilon, "optoncdt laser triangulation displacement sensors," 2016. [Online]. Available: <http://www.micro-epsilon.com/download>

[13] A. Simonian, "Feedback control for planar parallel magnetic manipulation," Master's thesis, Czech Technical University, Prague, 2014.

[14] P. Hammond and J. K. Sykulski, *Engineering electromagnetism: physical processes and computation*. Oxford University Press, 1994.

[15] L. Ljung, "System identification toolbox for use with MATLAB," 2007.

[16] M. Verhaegen and V. Verdult, *Filtering and system identification: a least squares approach*. Cambridge university press, 2007.

[17] J.-J. E. Slotine, W. Li, *et al.*, *Applied nonlinear control*. prentice-Hall Englewood Cliffs, NJ, 1991, vol. 199, no. 1.

[18] A. Megretski, "Lecture 13: Feedback linearization," 2016.

[19] A. Isidori, "Feedback linearization of nonlinear systems," *Control Handbook*, pp. 909–917, 1996.

[20] H. Khalil, "Nonlinear systems," 2002.

[21] F. L. Lewis and V. L. Syrmos, *Optimal control*. John Wiley & Sons, 1995.

[22] K. J. Åström and R. M. Murray, *Feedback systems: an introduction for scientists and engineers*. Princeton university press, 2010.

[23] E. Erdem, "Analysis and real-time implementation of state-dependent riccati equation controlled systems," Illinois, Tech. Rep., 2001.

[24] J. R. Cloutier, "State-dependent riccati equation techniques: An overview," in *American control conference*, New Mexico, 1997, pp. 932–936.

[25] H. Banks, B. Lewis, and H. Tran, "Nonlinear feedback controllers and compensators: a state-dependent riccati equation approach," *Computational Optimization and Applications*, vol. 37, no. 2, pp. 177–218, 2007.

[26] I. Chang and J. Bentsman, "Constrained discrete-time state-dependent riccati equation technique : A model predictive control approach," Tech. Rep., 2013.

[27] A. Bemporad, "Model predictive control : Basic concepts," Lucca, Italy, 2009.

[28] Z. Qu, *Robust control of nonlinear uncertain systems*. John Wiley & Sons, Inc., 1998.

[29] K. J. Åström and B. Wittenmark, *Adaptive control*. Courier Corporation, 2013.

[30] O. Sprangers, R. Babuška, S. P. Nagesh Rao, and G. A. Lopes, "Reinforcement learning for port-hamiltonian systems," *IEEE transactions on cybernetics*, vol. 45, no. 5, pp. 1017–1027, 2015.